Tunable Digital Metamaterial for Broadband Vibration Isolation at Low Frequency

Ziwei Wang, Quan Zhang, Kai Zhang, and Gengkai Hu*

A challenge for traditional elastic metamaterials is how to broaden the range of bandgaps at low frequency in a tunable way. This paper proposes a tunable digital elastic metamaterial fabricated by 3D-printing technology, consisting of a primary frame and auxiliary beams with embedded electromagnets. Switching electromagnets between the attaching (1 bit) and detaching (0 bit) modes activates different waveguides in the metamaterial. The underlying mechanism is investigated theoretically and experimentally. The hierarchical assemblies of unit cells allow programmable broadening of the metamaterial bandgap, providing new avenues for vibration isolation in many engineering fields.

Elastic metamaterials are artificial composites with various unusual properties,[1] like negative effective mass density,[2] negative effective modulus,[3] negative Poisson's ratio,[4] etc. Those features unavailable from nature materials make metamaterials quite attractive in advanced engineering applications,[5] such as vibration isolation,[6,7] wave guiding,[8,9] subwavelength focusing,[10] and invisible cloaking.[11] One notable characteristic is the capability to generate bandgaps at relatively low frequency ranges, due to local resonance of units embedded in cells.[2] Practically, traditional elastic metamaterials only operate at fixed frequency ranges with a single function due to the fixed microstructure, which limits potential applications. To break the restriction, elastic metamaterials need to be tunable when subjected to different external environments. An effective method to design tunable elastic metamaterials is provided by adjusting resonance frequency of local resonators. The corresponding mechanisms include piezo shunting,[12–14] structural deformation,[15,16] and shape memory effect.[17,18] However, these tuning methods require sophisticated design of local resonance units or overall structure, and the design concepts are challenging to trigger transformation of local resonators in simple ways, particularly at low frequency. On the other hand, hierarchical assemblies of unit cells in the metamaterial, created by manipulating the individual "artificial atoms" are expected to create novel metamaterials with effective macroscopic behavior. Tunable metamaterials can be fabricated by integrating hierarchical design methodology,[19] additive manufacturing solution,[20] digital technology,[21] etc. However, multifunctional tunable metamaterials fabricated by these advanced technologies are not currently available. We propose a new type of tunable digital elastic metamaterial, where the internal resonators within each unit cell can be switched by controlling the current of electromagnets at the tip end of the resonators. Programmable functionalities, such as wave guiding and isolating, are arbitrarily achievable in the metamaterial with appropriate coding mechanisms.

Starting with the proposed metamaterial as shown in **Figure 1**a, comprising a square structure with a 12 × 12 array of unit cells, where each unit cell consists of a square frame, two pairs of beams, and two electromagnets (see Figure 1b and Experimental Section for a detailed description). In each unit cell, a switch is connected with two electromagnets in series, forming a series circuit. All the series circuits are connected in parallel and powered by DC supply, so that each unit cell can be controlled independently. By switching the current in the desired cell, electromagnets can attach or detach from each other, transforming cell configuration between attaching (Att) and detaching (Det) modes (Figure 1c).

To investigate the propagation behavior of elastic wave in the metamaterial, experiments are conducted by first suspending the whole structure with strings linking the upper edge, keeping the plane coincident with the gravitational direction. A continuous out-of-plane harmonic excitation is then applied on the lattice edge by using an electrodynamic shaker (HEV-50, Nanjing Foneng, China), highlighted as the red line in Figure 1a. Three different structural configurations: all cells in Det mode, L shape route, and a bypass route, are achieved by controlling the corresponding cells into Att mode, marked with black circles in Figure 1d. The resulting wave propagation field is recorded using a scanning laser Doppler vibrometer (PSV-400, Polytec, Inc., Germany) by scanning the lattice response over a grid of points covering the whole metamaterial. The experimental root mean squared distributions of the velocity field corresponding to the three different configurations (Figure 1d) show waveguides at 60 Hz, consistent with the numerical simulations (Figure 1e). The wave only propagates along the route defined by cells in Att mode, and suffers severe attenuation in any deviation. Thus, a chain of Att mode unit cells behaves as a tunable waveguide in the structure.

The beams combined with the electromagnets in unit cell form an auxiliary structure attached to the cell frame, and behaves as a local resonator. The local resonance of the auxiliary introduces a bandgap, preventing elastic wave propagation. By attaching electromagnets, the boundary of the tip end of the internal resonator is changed from free to fixed, producing different resonant frequency of the internal resonator and hence bandgap of the metamaterial. To explain the fundamentals of this phenomenon, a 1D spring-mass lattice with internal resonators is considered by theoretical analysis and experiment, as shown in **Figure 2**.

Z. Wang, Q. Zhang, Dr. K. Zhang, Prof. G. Hu
School of Aerospace Engineering
Beijing Institute of Technology
Beijing 100081, China
E-mail: zhangkai@bit.edu.cn

DOI: 10.1002/adma.201604009

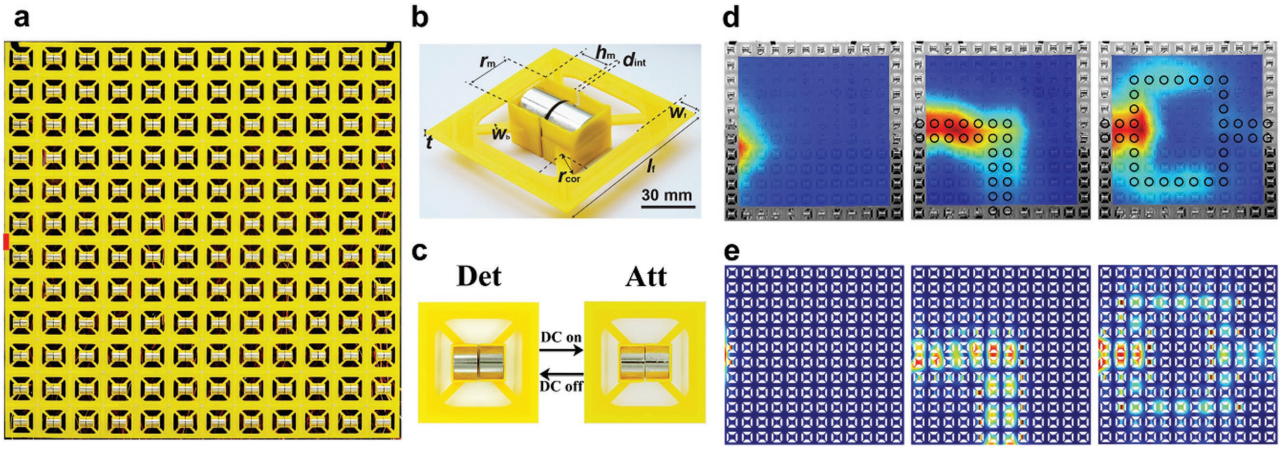

Figure 1. a) 3D printed metamaterial with 12 × 12 array of unit cells. b) A unit cell consisting of a square frame, two pairs of beams, and two electromagnets. c) Transformation between detaching (Det) and attaching (Att) configuration by DC switching. d) Experimental and e) numerical investigation of wave propagation in the metamaterial with all cells in Det mode, programmed L shape, and bypass route. The black circles represent the cells in Att mode.

Masses $m_1 = 145.9$ g are connected via a spring $k_1 = 135$ N m^{-1}, forming a series of identical cells with characteristic length $L = 170$ mm. When the current is off, no magnetic force will be generated between electromagnets (Figure 2a, Det mode). The internal resonator, consisting of a mass $m_2 = 88$ g connected with the outer mass through spring $k_2 = 135$ N m^{-1}, oscillates freely in the cell and is characterized with resonant frequency $f_R = 6.23$ Hz. When current is switched on, an attraction force appears between two electromagnets in the cell, and the internal resonator mass m_2 will be strongly attracted toward m_1, producing the configuration shown in Figure 2a, Att mode. Details of theoretical and experimental dynamic behavior of the lattice in Att and Det modes are provided in the Supporting Information.

Figure 2c shows both experimental and theoretical transmittance of the lattice in Det (red dots and red line) and Att mode (blue circles and blue dash line) modes. Lattice transmittance of Det mode has a severe drop from 5.5 to 8 Hz, which coincides with the bandgap range of the lattice in this configuration (indicated by the red area in Figure 2c). The negative effective

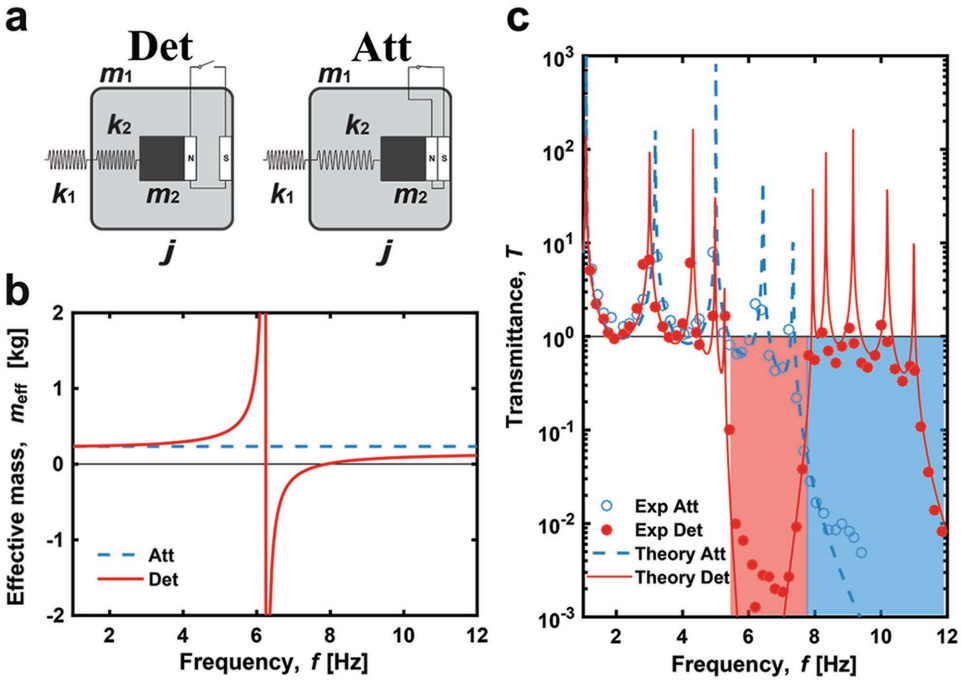

Figure 2. a) Schematic unit cell of 1D spring-mass lattice in detaching (Det) and attaching (Att) modes. b) Effective mass of unit cell in detaching (Det) and attaching (Att) modes. c) Experimental and theoretical transmittance of a 5 cell lattice in Det and Att modes.

mass region of the cell in Det mode (Figure 2b) also falls within that range, indicating the bandgap is due to negative effective mass, which is realized through the local resonant of the internal resonators.[22,23] There is no region of negative effective mass for the Att mode (Figure 2b), and lattice transmittance starts dropping from 7.7 Hz (Figure 2c, blue stop band). Thus, switching cells between Det and Att mode changes the resonant frequency of internal resonators, leading to tuning or broadening of the frequency range of bandgap.

Standard regular lattices with auxiliary cantilevers have shown the ability to forbid elastic waves from propagating within low frequency ranges, due to the local resonance of the auxiliary cantilevers.[6] **Figure 3**a shows that the significant complete bandgap from 59.5 to 106.1 Hz appears between second and third branch. The almost flat second branch is nearly equal to the first out of plane mode eigenfrequency of the internal resonator with fixed end, consisting of the electromagnets and beams. This indicates that the formation of the low frequency bandgap is due to the local resonance of the internal resonator. However, when the electromagnets are attached, the first out of plane mode eigenfrequency of the internal resonator changes, and consequently the complete bandgap from 59.5 to 106.1 Hz disappears (Figure 3b). Therefore, DC switching introduces structural transformation of the internal resonator, shifting the complete bandgap of the metamaterial. Thus, the wave only travels through the blocks in Att mode, being prohibited from Det mode blocks at 60 Hz, as seen in Figure 1d,e.

The unit cell of the proposed metamaterial can be switched between two states with corresponding bandgap on/off in specific range of frequency, coincidentally imitating the 0 and 1 bits of digital technology. The 0 bit represents a single cell in Det mode, while the 1 bit is a single cell in Att mode. Wave propagation is forbidden in 0 bits and allowed in 1 bits. This interesting parallelism enables the realization of coding digital metamaterials.[24] Traditional metamaterials are usually described by effective medium parameters on the macroscopic scale, referred to as analog metamaterials.[24] Comparing with this, digital metamaterials with a wide range of desired parameter value may be synthesized by combining and sculpting only two different materials, 0 and 1 bits, providing an excellent balance between complexity and simplicity. Spatial mixtures of such digital bits can produce digital metamaterial bytes (supercells) with higher degrees of freedom, leading to novel effective properties of the digital metamaterial. By coding 0 and 1 bits with designed sequences, the proposed tunable metamaterial helps achieve programmable smart metamaterials with different functionalities.

Since every unit cell acts as a digital bit with switchable 0 and 1 states, supercells, composed of multiple unit cells, may exhibit even more diverse behaviors. Consider a 3×3 supercell with different 1 and 0 bit sequences. There are 2^9 possible sequences for the 3×3 supercell, but only 26 are independent due to the structural symmetry. **Figure 4** shows frequency ranges of bandgap as a function of the number of 0 bits in the 3×3 supercell. The bandgap is produced via local resonance of auxiliary structures, and can be verified by checking vibration modes of the lower band of the bandgap at symmetry points of the irreducible Brillouin zone (e.g., (a), (e), (h), and (j) in Figure 4). When the supercell is filled with 1 bits, i.e., the number of 0 bits is zero, the frequency range of bandgap is minimum. With increasing of 0 bits number, the average frequency range of bandgap monotonically increases from 0 to 45 Hz. In addition, the distribution of 0 bits in the supercell also affects the frequency range of bandgap. For example, there are five possible distributions with four 0 bits, varying frequency range of bandgap from 20.6 to 34.3 Hz. The lower boundary for the bandgap of all cases changes from 59.5 (all 0 bits) to 97.8 Hz (all 1 bits), whereas deviations of the upper boundary are small. Therefore, hierarchical manipulation of the unit cells in our proposed metamaterial shows a remarkable ability to adaptively broaden the bandgap.

The proposed tunable metamaterial can be deployed as a surface coating to manipulate wave propagation of flexible

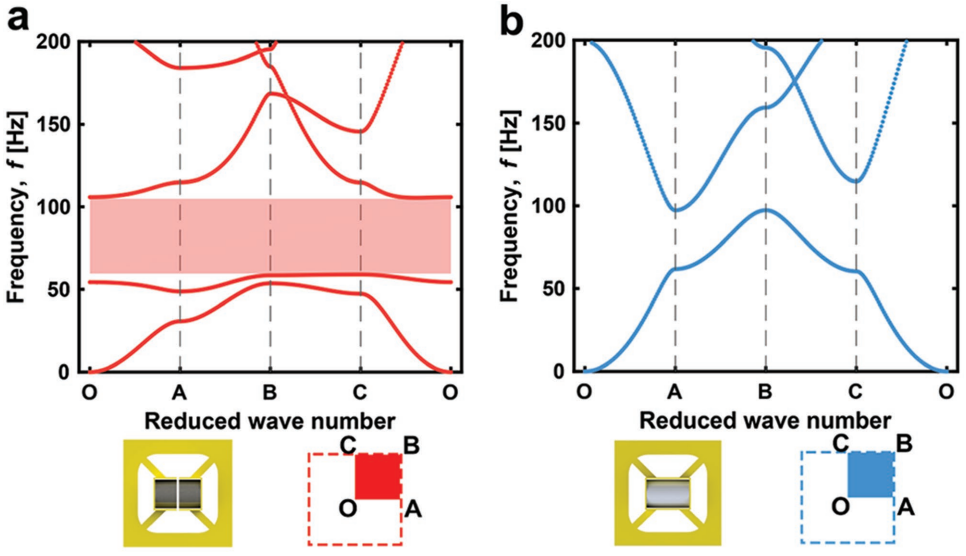

Figure 3. Band structures of the metamaterial for a) detaching (Det) and b) attaching (Att) modes.

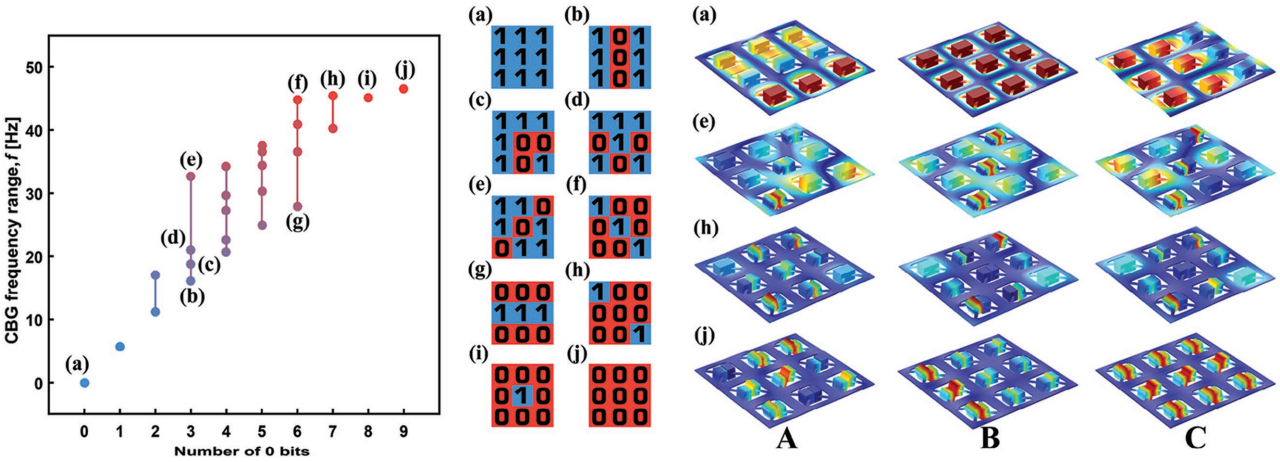

Figure 4. Complete bandgap (CBG) frequency ranges of 3 × 3 supercells for 26 independent configurations. Configurations of points (a–j) are presented. Vibration modes of the lower band of the bandgap at symmetry points of the irreducible Brillouin zone (A, B, C) are shown for configurations (a), (e), (h), and (j), featuring local resonance of local resonators.

structure. A homogenous flexible structure is incapable of manipulating wave propagation, but this limitation can be broken by coating the proposed metamaterial onto the surface of flexible structure by using additive manufacturing technology. The tunable metamaterial can be adhered to the surface of flexible substrate as a thin layer, while still providing sufficient space to allow the internal resonators to vibrate, as shown in **Figure 5**a. Arbitrary waveguides can be designed in the combined structure using appropriate coding mechanisms to sequence the 0 and 1 bits as desired, such as the U and S curves shown in Figure 5b. Thus, wave propagation within the flexible structure can be controlled by programming the metamaterial waveguide on its surface.

Based on tunable metamaterial, we propose the concept of a multi-functional intelligent device by attaching thin piezoelectric polyvinylidene fluoride (PVDF) films on the surface of the auxiliary beams, as shown schematically in Figure 5c. When excitation in the frequency range of bandgap is applied to the device, all the auxiliaries resonate, producing first mode deformed shape. The mechanical waves will be localized and the wave energy will transfer into kinetic energy of the auxiliary structures. The piezoelectric PVDF films on auxiliary beams then convert the kinetic strain energy into electricity. From the resonating of the auxiliary structures, harvested electricity power can energize electromagnets or magneto–electro materials at the tip end of the structures in the marginal cells of the device, switching the states into 1 from 0, forming a circular waveguide. Thus, the wave will be manipulated into the corner of the device and absorbed by damping materials. Consequently, an internal environment is generated free from

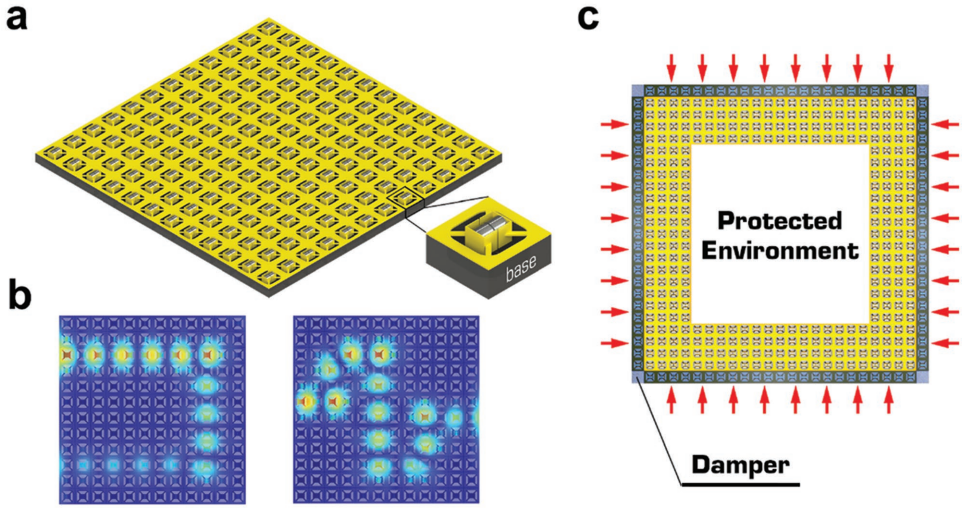

Figure 5. a) Flexible base coated with proposed tunable metamaterial surface is able to b) control wave propagation within it. c) An intelligent device with piezoelectric PVDF film on the auxiliary beams isolates harmful vibration and creates a protected internal environment, showing self-sensing, self-responding and self-powering features.

externally applied mechanical loads by insulating potentially harmful excitations. The proposed intelligent multifunctional device is self-sensing, self-responding, and self-powering, and could be applied extensively to control micro or macroscopic structural vibrations.

In summary, we proposed a tunable digital metamaterial, consisting of a primary lattice and auxiliary beams with embedded electromagnets. Desirable waveguides can be achieved in the metamaterial by controlling the current to the electromagnets of each cell. By switching unit cells between Det (0 bit) and Att modes (1 bit), the bandgap corresponding to a low resonance frequency of the internal resonator can be open or closed, due to variation in the boundary condition of the beams. Moreover, introducing a coding mechanism allows the frequency range of bandgap to be broadened by increasing the number of 0 bits within a supercell, and fine tuning the distribution. The proposed metamaterial can also improve wave propagation control for flexible structures, and provide the opportunity for new intelligent devices to achieve vibration isolation.

Experimental Section

Description of the Proposed Metamaterial: The side length, l_f; thickness, t; and width, w_f, of the unit cell frame are 75, 1.9, and 10 mm, respectively; and the radius, r_{cor}, of the internal filleted corners is 13.8 mm. Two pairs of beams were connected to the frame in the direction of the diagonals of the square cell with size 17.7 mm × 5 mm (length × width, w_b) and the thickness was as same as the frame. Every unit cell in the metamaterial was fabricated using a 3D printer (Replicator 2X, MakerBot, USA) with printing polylactide, and cylindrical electromagnets with radius r_m = 20 mm and height h_m = 15 mm, were placed in the cell with their axes lying in the middle plane of the frame. The opposite poles of the electromagnets facing each other were separated by d_{int} = 1.5 mm. The electromagnets are rated for 12 VDC, and the needed current is 0.5 A for state switching.

Supporting Information

Supporting Information is available from the Wiley Online Library or from the author.

Acknowledgements

The authors thank the National Natural Science Foundation of China (Grants No. 11202025 and No. 11290153) for financial support. The authors thank Prof. Li Zheng, Liu Yongquan, Yi Jianling, and Chen Han for help in calculation and experiments.

Received: July 28, 2016
Revised: August 29, 2016
Published online: September 22, 2016

[1] M. I. Hussein, M. J. Leamy, M. Ruzzene, *Appl. Mech. Rev.* **2014**, *66*, 40802.
[2] Z. Liu, X. Zhang, Y. Mao, Y. Y. Zhu, Z. Yang, C. T. Chan, P. Sheng, *Science*. **2000**, *289*, 1734.
[3] N. Fang, D. Xi, J. Xu, M. Ambati, W. Srituravanich, C. Sun, X. Zhang, *Nat. Mater.* **2006**, *5*, 452.
[4] R. S. Lakes, *Adv. Mater.* **1993**, *5*, 293.
[5] M. H. Lu, L. Feng, Y. F. Chen, *Mater. Today* **2009**, *12*, 34.
[6] S. Gonella, A. C. To, W. K. Liu, *J. Mech. Phys. Solids* **2009**, *57*, 621.
[7] J. Mei, G. Ma, M. Yang, Z. Yang, W. Wen, P. Sheng, *Nat. Commun.* **2012**, *3*, 756.
[8] M. B. Assouar, M. Senesi, M. Oudich, M. Ruzzene, Z. Hou, *Appl. Phys. Lett.* **2012**, *101*, 1.
[9] M. Oudich, M. B. Assouar, Z. Hou, *Appl. Phys. Lett.* **2010**, *97*, 18.
[10] M. Ambati, N. Fang, C. Sun, X. Zhang, *Phys. Rev. B: Condens. Matter Mater. Phys.* **2007**, *75*, 1.
[11] S. A. Cummer, D. Schurig, *New J. Phys.* **2007**, *9*, 45.
[12] A. Bergamini, T. Delpero, L. De Simoni, L. Di Lillo, M. Ruzzene, P. Ermanni, *Adv. Mater.* **2014**, *26*, 1343.
[13] R. Zhu, Y. Y. Chen, M. V. Barnhart, G. K. Hu, C. T. Sun, G. L. Huang, *Appl. Phys. Lett.* **2016**, *108*, 11905.
[14] F. Casadei, T. Delpero, A. Bergamini, P. Ermanni, M. Ruzzene, *J. Appl. Phys.* **2012**, *112*, 064902.
[15] S. Babaee, N. Viard, P. Wang, N. X. Fang, K. Bertoldi, *Adv. Mater.* **2016**, *28*, 1631.
[16] P. Wang, F. Casadei, S. Shan, J. C. Weaver, K. Bertoldi, *Phys. Rev. Lett.* **2014**, *113*, 014301.
[17] Q. Zhang, D. Yan, K. Zhang, G. Hu, *Sci. Rep.* **2015**, *5*, 8936.
[18] Q. Zhang, K. Zhang, G. Hu, *Sci. Rep.* **2016**, *6*, 22431.
[19] C. Cao, H. F. Chan, J. Zang, K. W. Leong, X. Zhao, *Adv. Mater.* **2014**, *26*, 1763.
[20] J. H. Lee, C. Y. Koh, J. P. Singer, S. J. Jeon, M. Maldovan, O. Stein, E. L. Thomas, *Adv. Mater.* **2014**, *26*, 532.
[21] C. Liaskos, A. Tsioliaridou, A. Pitsillides, I. F. Akyildiz, N. V. Kantartzis, A. X. Lalas, X. Dimitropoulos, S. Ioannidis, M. Kafesaki, C. M. Soukoulis, *IEEE Circuits Syst. Mag.* **2015**, *15*, 12.
[22] S. Yao, X. Zhou, G. Hu, *New J. Phys.* **2008**, *10*, 043020.
[23] H. H. Huang, C. T. Sun, G. L. Huang, *Int. J. Eng. Sci.* **2009**, *47*, 610.
[24] C. Della Giovampaola, N. Engheta, *Nat. Mater.* **2014**, *13*, 1115.